

## The Application of an Activated Carbon Supported Cu-Ce/AC Oxide Anode on the Electrocatalytic Degradation of Phenol

Jun-e Qu<sup>1,2</sup>, Shu Zhou<sup>2</sup>, Hairen Wang<sup>1,2,\*</sup>, Zhiyong Cao<sup>1,2</sup>, Hongfang Liu<sup>3</sup>

<sup>1</sup> Faculty of Materials Science and Engineering, Hubei University, WuHan,430062, PR China

<sup>2</sup> Ministry-of-Education Key Laboratory of Green Preparation and Application for Functional Materials, Faculty of Materials Science & Engineering, Hubei University, Wuhan, 430062, China

<sup>3</sup> Department of Chemistry, HuaZhong University of Science and Technology, Wuhan 430074, Hubei, China

\*E-mail: [whr9999whr@163.com](mailto:whr9999whr@163.com)

Received: 22 June 2017 / Accepted: 4 August 2017 / Published: 12 September 2017

---

The Cu-AC (AC: activated carbon) and Cu/Ce-AC composite materials were synthesized using a one-pot sol-gel method. The surface microstructure and composition of the resulting samples were characterized by Brunauer–Emmett–Teller (BET) specific surface area analysis, scanning electron microscopy/energy dispersive x-ray(SEM/EDX), and XPS(X-ray photoelectron spectroscopy) compared to pure AC. Finally, the electrochemical catalytic activity of the prepared materials for the oxidative degradation of phenol were contrastively studied. It was found that the Cu/Ce-AC catalyst had larger surface area, greater  $pH_{PZC}$  value (pH value at the point of zero charge), stronger ability to chemisorb active oxygen, and more possible forms of higher oxides generated from chemisorbed hydroxyl radicals, than AC and Cu/AC. These factors synthetically resulted in its more prominence electro catalytic activity for phenol degradation compared to AC and Cu/AC. The 50min continuous electrochemical degradation for phenol by using Cu/Ce-AC achieved over 97% COD and 80% TOC removals at initiate phenol concentration =504mg/L, temperature = 25°C, pH = 3.0 and  $j = 80 \text{ A}\cdot\text{m}^{-2}$ . The considerable electro catalytic performance of Cu-Ce/AC material makes it a promising anode for electrochemical treatment of organic pollutants in aqueous solution.

---

**Keywords:** phenol, sol-gel method, electrochemical degradation, Cu-Ce/AC anode

### 1. INTRODUCTION

Phenol and its derivatives are toxic even at extremely low concentrations but stable to the biodegradation. In the last decades, various catalysts for chemical degradation had been developed and used in the degradation of phenol [1-4]. Homogenous catalysts, for example soluble salts of Fe, Cu, Ni,

Co, Ce and Mn elements etc., were proved to have good catalytic activity [5]. However, the using of these soluble salts makes troublesome procedure of removing metal ions from wastewater. To overcome this drawback, heterogeneous catalysts based on supported or unsupported metal oxides (e.g., Cu, Zn, Mn, Ti) and noble metals (e.g., Ru, Pt, Pd, Ag and Rh) have been developed for phenol treatment [6-8]. But in these cases, the chemical degradation must be performed with adding the expensive  $H_2O_2$  (or other oxidant) to the wastewater solution. While in acidic or neutral solution, the metal oxides with redox properties react with  $H_2O_2$  to generate hydroxyl radicals, which could directly oxidize the organic molecules. Without  $H_2O_2$  in the solution, the degradation rate of organic molecules was generally poor.

Another promising method for degrading refractory organic pollutants in water is electrochemical oxidation because of its strong oxidation performance, easy implementation, and compatibility of environmental protection [9]. The electro-catalytic oxidation technology was usually used in wastewater to treat organic and poisonous contamination, especially for the degradation of non-biodegradable organic pollutants [10]. However, the oxidation efficiency of organic pollutants during electrochemical oxidation process is strongly dependent on the material of anodes. Among typical anodes materials including graphite [11], noble metal (e.g., Pt) [12], metal oxide (e.g.,  $PbO_2$ ,  $SnO_2$ ,  $RuO_2$ ,  $IrO_2$ ,  $CuO$ ,  $TiO_2$ ) [13-17], and boron-doped diamond (BDD) [18], metal oxide anode has attracted much attention because of its electro-catalytic property, relative low cost and stability in the electrolytic.

It is well known that rare earth oxides are powerful catalysts in oxidation reactions. For example, doping of  $Er_2O_3$ ,  $Gd_2O_3$ ,  $La_2O_3$  and  $Ce_2O_3$  into the  $PbO_2$  film could enhance the degradation of 4-chlorophenol [19]. The  $PbO_2$  electrodes modified with rare earth (La and Ce) prepared by electrodeposition technique indicated a dense structure and a preferred crystalline orientation, which were beneficial to pollutant degradation [20]. After being doped by oxides of Ce and Ru, ternary  $SnO_2$  based oxides anode (Ce-Ru- $SnO_2$ ) indicated a higher electrochemical activity for degradation of nitro-phenol [21]. However, to the best of our knowledge, there are fewer reports on degradation of organic pollutants by using activated carbon (AC) supported metal oxides as electrode materials.

In this work, the low-cost AC with higher surface area was used as a catalytic support, and metal oxides of Cu and Ce were loaded to the AC matrix by sol-gel method to get granular Cu/AC and Cu-Ce/AC composite materials. The electrochemical degradation of phenol by AC, Cu/AC and Cu-Ce/AC materials assembled in the stainless steel wire mesh working as anode were contrastively studied in terms of chemical oxygen demand (COD) and total organic carbon (TOC). The composition and micro-structure of the anode materials were characterized by using BET, SEM-EDS, and XPS.

## 2. EXPERIMENTAL

### 2.1. Preparation of Cu-AC and Cu/Ce-AC anode materials

Activated carbon (AC) raw materials with the mesh number of 8 to 16 (2.36mm-1mm) were treated with dilute nitric acid solution for 24 h at 25°C. The oxidized AC were extensively washed with

distilled water to neutral pH, dried in an oven at 100°C for 6 h, and then were used as support materials. The pure AC materials used in all the control experiments were the nitric acid-treated AC. The bimetallic Cu/Ce-AC supported catalyst were prepared by one-pot sol-gel method. A homogenous mixture solution containing  $0.3\text{mol}\cdot\text{L}^{-1}$   $\text{Cu}(\text{NO}_3)_3$ ,  $3\text{mmol}\cdot\text{L}^{-1}$   $\text{Ce}(\text{NO}_3)_3$  and  $0.6\text{mol}\cdot\text{L}^{-1}$  citric acid was prepared, and then a certain amount of treated AC was added into the aqueous solution. Afterwards, aqueous ammonia (28 wt%) was added dropwise into the heterogeneous mixture solution at room temperature with vigorous magnetic stirring until the desired pH 6.5 reached. Then, the resulting mixture solution was transferred into a water bath at 80°C and kept for 48h. After being cooled to room temperature, the precursor of AC supported metallic oxides were collected and calcined in air at 500°C for 5h. Finally, the prepared composite material was signed as Cu/Ce-AC.

The synthesis route of Cu/AC catalyst was the same as that for Cu/Ce-AC, except that no  $\text{Ce}(\text{NO}_3)_3$  was added.

## 2.2. Characterization of composite anode materials

Specific surface areas of supported catalysts were determined by nitrogen gas adsorption apparatus (Micromeritics Inc. ASAP 2020 HD88) at -196°C. Before gas adsorption measurement, all samples were degassed at 250°C in a vacuum  $10^{-3}$  Torr for 4h. Surface areas and micropore volumes of samples were determined using the Brunauer-Emmett-Teller (BET) and Dubinin-Radushkevich (D-R) equations.

The pH values at point of zero charge,  $\text{pH}_{\text{PZC}}$ , of AC, Cu/AC and Cu-Ce/AC were determined according to the pH drift method [22,23]. A 0.01M NaCl solution was prepared using deionized water. Ten different standard solutions having pH ranging from 2 to 11 were prepared using the 0.01M NaCl by adding 0.1 M HCl or 0.1 M NaOH solutions. 0.05 g of sample was added to 20mL of each solution, and stirred 48h to reach equilibrium. Blank experiments (without addition of samples) were also performed for each pH and the values measured after 48 h are considered as the initial pH. The  $\text{pH}_{\text{PZC}}$  value of each sample was determined by intercepting the obtained final pH vs. initial pH curve with the straight line final pH = initial pH.

The microstructure and composition of anode materials were examined using scanning electron microscope (SEM-JEOL JSM6510LV) equipped with energy dispersive spectrometry (EDS). X-ray photoelectron spectra (XPS) were recorded at room temperature by using Thermo Fisher Scientific 250Xi analyzer with a magnesium anode for  $\text{K}\alpha$  ( $h\nu=1486.6\text{eV}$ ) radiation.

## 2.3. The electrochemical degradation of phenol

In order to get considerable surface areas, a certain amount of AC, Cu-AC, Cu/Ce-AC materials were assembled into tailor-made anode baskets using stainless steel wire mesh, respectively. The apparent working surface area of the anode was about  $50\text{cm}^2$ . A single compartment electrochemical glass cell was employed to perform phenol degradation using a homemade PAN-carbon felt air diffusion electrode as cathode(prepared according to the reported procedures[24]) and

the prepared composite material as anode. The electrolysis experiments were performed in galvanostatic mode, controlled by an electro-chemical workstation. The gap between the cathode and anode was 4 cm. Oxygen was bubbled from the roof of the reactor for the entire duration of the reaction at  $0.1\text{m}^3\cdot\text{L}^{-1}$  in order to keep the solution saturated in oxygen gas. Additionally, the solution was mechanically stirred during the whole degradation process. The initial phenol concentration was  $504\text{mg}\cdot\text{L}^{-1}$  (300 mL), and  $1\text{g}\cdot\text{L}^{-1}$   $\text{Na}_2\text{SO}_4$  was used as a supporting electrolyte. Electrolysis was carried out at initial pH 3.0, adjusted by adding drops of 0.1M  $\text{H}_2\text{SO}_4$  or 0.1M NaOH at room temperature.

The decolourization and mineralization of phenol was investigated by total organic carbon (TOC) removal and chemical oxygen demand (COD) analysis.

### 3. RESULTS AND DISCUSSION

#### 3.1 Microcharacterization

The results regarding to pore structure and surface area of the three kinds of materials, namely AC, Cu-AC and Cu/Ce-AC were shown in table 1. It revealed that original AC had higher BET surface area and larger total pore volume than Cu-AC. On the contrary, Cu/Ce-AC had the highest BET surface area and total pore volume among the three materials, suggesting that the added Ce rare earth element changed the surface properties of AC and Cu/AC samples obviously.

**Table 1.** Surface characteristics of AC, Cu-AC and Cu/Ce-AC.

Sample	BET surface Area	Total pore volume	Average pore size
	( $\text{m}^2/\text{g}$ )	( $\text{cm}^3/\text{g}$ )	(nm)
AC	695.453	0.363	2.087
Cu-AC	632.214	0.311	1.967
Cu/Ce-AC	816.957	0.392	2.098

The SEM topographies of AC, Cu-AC and Cu/Ce-AC materials were shown in Figure1. As in Figure1(a), AC showed smooth surface with a large number of micropores. Aggregation of the particles with irregular shapes could be seen on the surface of Cu-AC catalyst from Figure1 (b). So the reduction in the surface area and pore volume of Cu-AC could be explained by the introduction of copper oxide with uneven sizes, and the big particles of copper oxide might lead to active sites occlusion inside the pores and on the surface of AC [25-27]. However, in Figure1 (c) the size of the uniformly distributed particles on the surface of Cu/Ce-AC catalyst was much smaller compared with that of Cu-AC catalyst. Obviously, the highly uniform dispersion of the particle with smaller size is the reason for the largest specific surface area of Cu/Ce-AC among these three materials as shown in Table 1.

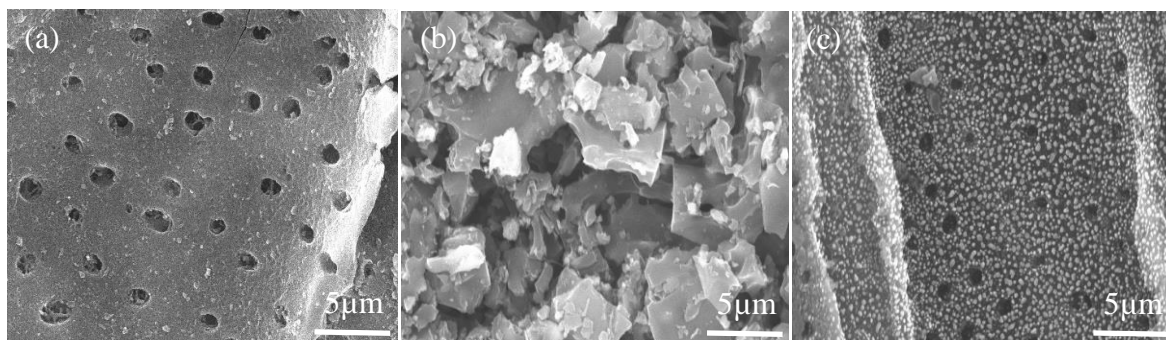


**Figure 1.** SEM images of AC(a) , Cu-AC(b) and Cu/Ce-AC(c).

**Table 2** The atom fractions (At.%) of main elements in the AC, Cu-AC , Cu/Ce-AC materials as determined from EDS analysis.

Sample	C	O	Cu	Ce
AC	94.50	5.50	—	—
Cu-AC	93.95	4.02	2.04	—
Cu/Ce-AC	93.49	4.71	1.72	0.09

The elementary composition of AC, Cu-AC and Cu/Ce-AC analyzed by EDS were shown in Table 2. The blank AC surface mainly showed C and O elements. And on the surface of Cu-AC, Cu was examined also. Cu/Ce-AC surface verified the existence of modicum Ce other than C, O and Cu elements. The detected C on both surface of Cu-AC and Cu/Ce-AC mainly arised from active carbon base. The result clearly indicated that the copper oxide, and composite of copper oxide and cerium oxide have been successfully bounded on the surfaces of AC in Cu-AC and Cu/Ce-AC catalysts, respectively.

XPS analysis was performed to reflect the composition and chemical elementary state of the sample surface. The Cu2p, Ce3d, O1s XPS spectra of the composite catalyst materials were deconvoluted into the component peaks as shown in Figure 2, and the ratios of these peaks were calculated as shown in Table 3.

For the Cu 2P spectra of Cu-AC and Cu/Ce-AC samples, the components at 932.6eV and 952.5eV could be assigned to Cu 2p<sub>3/2</sub> and 2p<sub>1/2</sub> peaks of Cu<sub>2</sub>O, and at 933.7 eV and 953.6 eV assigned to the Cu 2p<sub>3/2</sub> and Cu 2p<sub>1/2</sub> peaks for the CuO, respectively[28].The shake-up satellite peaks of the Cu 2p<sub>3/2</sub> and Cu 2p<sub>1/2</sub> at around 942.0 eV and 961.9 eV also confirm the formation of CuO [29,30]. As shown by the data in Table 3, Cu<sup>2+</sup> oxidation state was predominant and the content ratio of Cu<sup>2+</sup>/Cu<sup>+</sup> is 78.48/21.52.

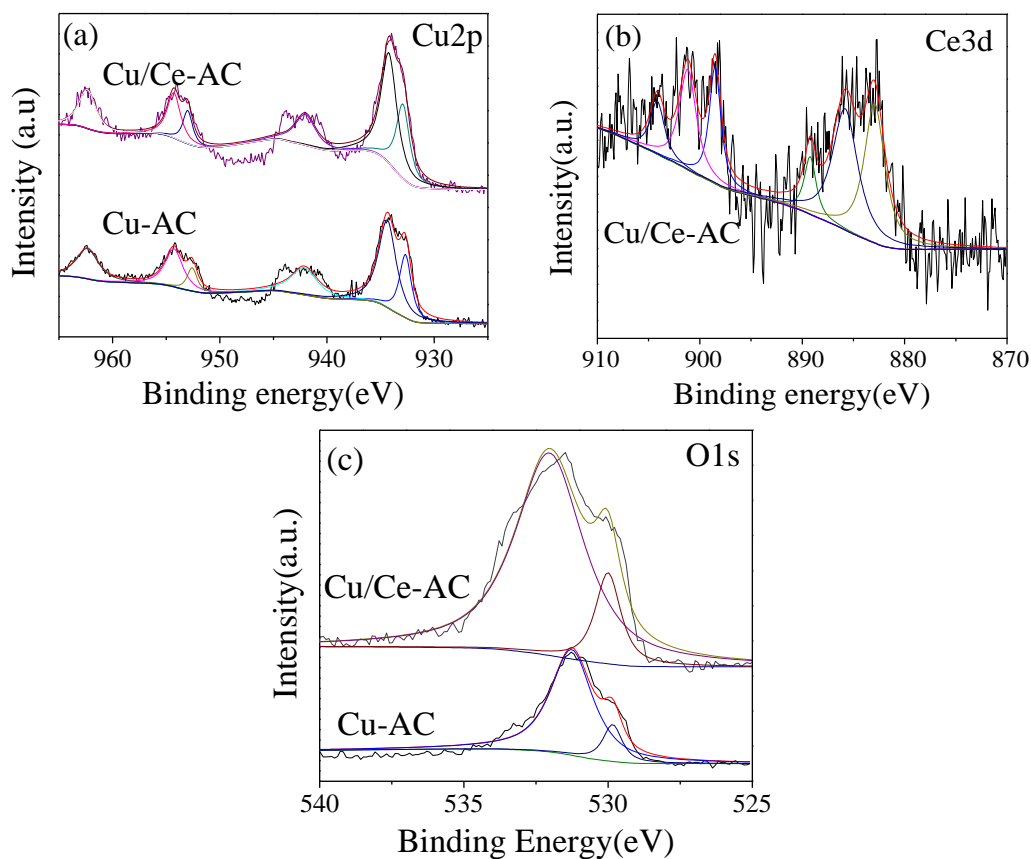


**Figure 2.** Fitted XPS Cu 2p(a), Ce 3d (b),and O1s(c) spectra of Cu-AC and Cu/Ce-AC catalysts.

Ce 3d XPS spectra of Cu/Ce-AC were deconvoluted into six peaks which have been attributed to the contributions of Ce  $3d_{5/2}$  and Ce  $3d_{3/2}$  spin-orbit components. The photoelectron peaks at about 882.93eV and 904.15eV represent for the existence of  $Ce^{3+}$  species[29], whereas the other four photoelectron bands at 885.81eV, 889.22eV, 898.50eV and 901.17eV can be assigned to the presence of  $Ce^{4+}$  ions[29,31]. The dominating valence of Ce in the Cu/Ce-AC sample was +4, and the calculated content ratio of  $Ce^{4+}/Ce^{3+}$  is 65.14/35.86 as displaced in Table 3.

The asymmetric and broad O1s XPS spectra of Cu-AC and Cu/Ce-AC could be divided into two peaks respectively. The peak at 531-533eV was attributed to the chemisorbed oxygen (denoted as  $O_{\beta}$ ) and another one at 529-530eV was attributed to characteristic lattice oxygen (denoted as  $O_{\omega}$ ) [32, 33]. Obviously, higher content ratio of chemisorbed oxygen( $O_{\beta}$ ) was found in Cu/Ce-AC sample than in Cu/AC as shown in Table 3. What is more, as shown by Figure 2(c), the peak area of  $O_{\beta}$  in Cu/Ce-AC sample was much greater than that of Cu/AC sample. According to the literature, the chemisorbed oxygen in the oxygen deficient regions which have higher mobility than lattice oxygen, can actively take part in the oxidation process and greatly contribute to the catalyst activity [34,35]. So the stronger ability to chemisorb oxygen on the surface of Cu-Ce/AC can be expected to enhance the performance of the anode for phenol degradation.

**Table 3.** The content ratios(%) of different chemical state of Cu, Ce and O elements in the anode materials.

Anode	Cu		Ce		O	
	Cu <sup>2+</sup>	Cu <sup>+</sup>	Ce <sup>4+</sup>	Ce <sup>3+</sup>	O <sub>α</sub>	O <sub>β</sub>
Cu-AC	78.48	21.52	—	—	17.19	84.25
Cu/Ce-AC	74.66	25.44	65.14	35.86	14.14	88.14

### 3.2 Degradation performance

#### 3.2.1 Removing of phenol

The effect of different electrode materials (AC, Cu/AC, Cu-Ce/AC) on the degradation of 504mg/L phenol in 1g/L Na<sub>2</sub>SO<sub>4</sub> solution was investigated at 300ml volume, pH 3, and air flow rate of 0.1m<sup>3</sup>/h, with or without applying outside current of 400mA. And The COD removal efficiencies as function of degradation time were shown in Figure 3 and Figure 5.

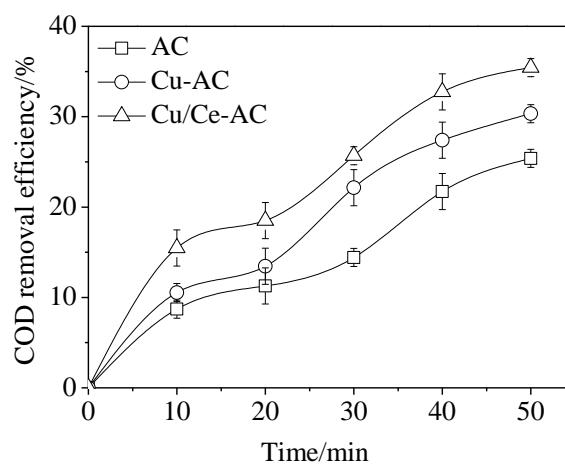


**Figure 3.** The effect of different materials on the COD removal efficiency under condition without external electrical supply.

In case of Figure 3, AC, Cu/AC and Cu/Ce-AC materials assembled in the stainless steel basket were placed in the phenol solution respectively without applying outside current. The COD removal efficiency, arising mainly from physical adsorption[36], could reach 25.39%, 30.34%, 35.43% in 50min, respectively. The removal efficiency order was in accordance with their measured pH<sub>PZC</sub> values as displaced in Figure 4 (AC: 2.82, Cu/AC:5.13, Cu-Ce/AC: 5.87). At higher pH<sub>PZC</sub> value, the surface of the adsorbent will exhibit higher positive surface charges, and positive charges could favor adsorption of aromatic compounds [23]. So the higher the pH<sub>PZC</sub> value, the more phenol molecules could be removed from the solution.

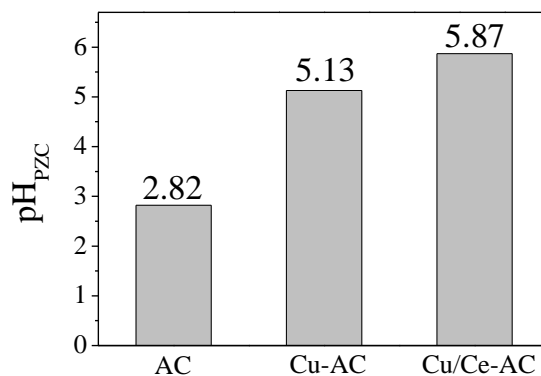


**Figure 4.** The  $\text{pH}_{\text{PZC}}$  values of AC, Cu/AC and Cu-Ce/AC materials measured in 0.01M NaCl solutions containing  $2.5 \text{ g}\cdot\text{L}^{-1}$  AC, Cu/AC and Cu-Ce/AC, respectively.

And in case of Figure 5, stainless steel baskets filled with AC, Cu-AC and Cu/Ce-AC were employed as anodes respectively, then the phenol solution was treated by electrolysis degradation with applying constant current of 400mA between the anode and the air diffusion cathode. COD removal efficiencies of AC, Cu-AC and Cu/Ce-AC anodes could reach 40.58%, 80.34%, 97.88% in 50min, respectively, which were much higher than the values under condition without external electrical supply. And the Cu/Ce-AC composite anode exhibited the highest value approaching 98%, proving that there existed synergistic effect between electrolysis and catalysts in the degradation of phenol.

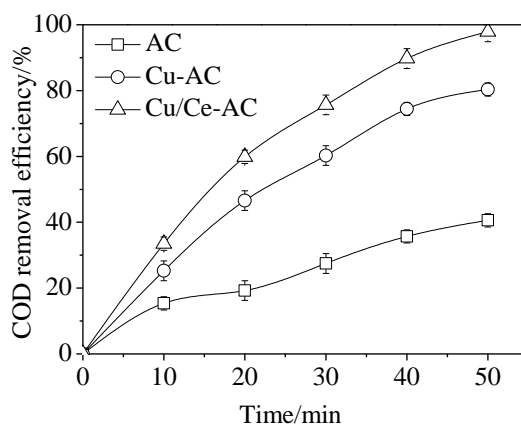


**Figure 5.** The effect of different materials on the COD removal efficiency under condition with external electrical supply.

Similar trends were observed for TOC tests. Figure 6 showed that, while compared with degradation without external electrical supply(Figure 6(a),(b),(c)), TOC removal efficiencies were greatly enhanced (Figure 6(d),(e),(f)) when AC, Cu-AC and Cu/Ce-AC composite anodes were used for electrochemical degradation. Consequently, based on the above results, electro-catalytic oxidation degradation by using Cu/Ce-AC composite anode was recommended as a suitable process for degradation of phenol, which could achieve 97.88% COD removal efficiency and 80.26% TOC removal efficiency.

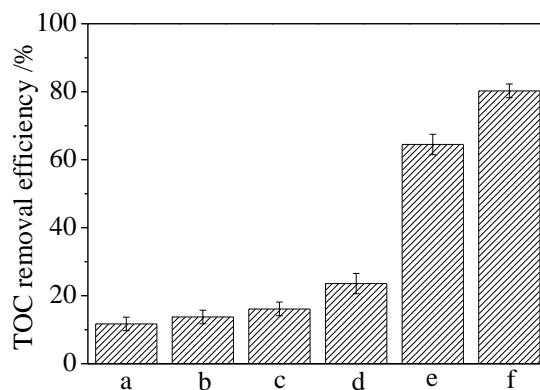
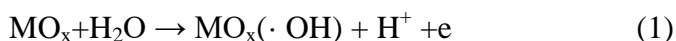


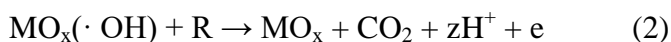
**Figure 6.** The effect of different materials and impressed current on TOC removal efficiency: treatment without external electrical supply by AC(a), Cu-AC(b) and Cu/Ce-AC(c); treatment with external electrical supply by AC(d), Cu-AC(e) and Cu/Ce-AC(f).

### 3.2.2 Possible electrochemical degradation mechanism

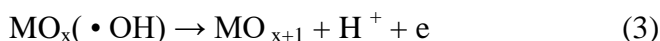
According to the mechanism proposed by Simond et al[37], metal oxide anode materials for electrochemical degradation of organic molecules have been classified as ‘active’ or ‘non-active’ electrodes[38,39], depending on their chemical nature. On the surface of both kinds of electrode ( $MO_x$ ), the first step happened is the formation of adsorbed hydroxyl radicals ( $\cdot OH$ ) from water discharge



With regard to non-active electrodes (such as  $SnO_2$ ,  $PbO_2$ ), the adsorbed strong oxidizing agent  $\cdot OH$  radicals can result in complete electrochemical oxidation of the organic molecule to  $CO_2$



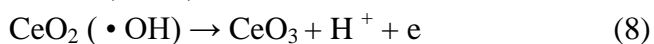
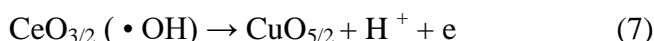
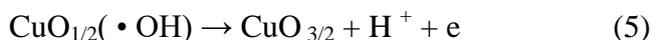
On the other hand, for active electrodes (such as  $RuO_2$ ,  $IrO_2$ ), except the direct electrochemical oxidation, the adsorbed  $\cdot OH$  can go on to form a higher oxide ( $MO_{x+1}$ ).



The oxidizing capacity of  $MO_{x+1}$  is not so strong as  $\cdot OH$  and only partial oxidation of the organic in solution to RO occurs.



As referred to this work, the XPS result has disclosed the existence of both CuO and  $Cu_2O$  in the Cu/AC and Cu-Ce/AC anodes, and  $CeO_2$  and  $Ce_2O_3$  in the Ce containing Cu-Ce/AC anode. So for the prepared Cu-Ce/AC composite electrode, more forms of higher oxide ( $MO_{x+1}$ ) generated from chemisorbed  $\cdot OH$  can be obtained compared with electrode containing metal elements only with single valence, as shown by the following equations (equation 5 to equation 8):



The more reaction paths will benefit the active electrode process for acquiring  $\text{MO}_{x+1}$ . Then it can be speculated that inactive and active processes are both involved for the Cu/AC and Cu-Ce/AC electrodes.

In addition, except for the aforementioned inactive and active processes,  $\text{Fe}^{2+}$  ions could be formed in the solution during the anodic electrochemical dissolution of the stainless wire mesh. As the well known Fenton reaction[40,41], the  $\text{Fe}^{2+}$  ions could react with the  $\text{H}_2\text{O}_2$  molecules arising from reduction of oxygen on the cathodic surface, and then to generate hydroxyl radicals ( $\cdot\text{OH}$ ) also. Some of hydroxyl radicals ( $\cdot\text{OH}$ ) generated from  $\text{H}_2\text{O}_2$  could chemically oxidized the organic molecules directly, and some could move to the anode surface and be involved in the inactive and active processes. However, under the condition with applied large direct current on the cell, the electrochemically produced hydroxyl radicals( $\cdot\text{OH}$ ) should be the dominant adsorbed hydroxyl radicals ( $\cdot\text{OH}$ ) on the anode surface, and the dominant degradation mechanism should be electrochemical oxidation reaction other than chemical oxidation and physical adsorption.

For the prepared Cu-Ce/AC anode, the grain refinement effect accompanying with increasing the specific surface area and higher ability to adsorb more active oxygen brought by adding Ce has been revealed by SEM and XPS studies, as similar as the reported Ce doping behavior for metal oxide electrodes using as anodes for pollutant degradation (such as Ti/ $\text{PbO}_2$ [42], Ti/ $\text{SnO}_2$ [43], and Ru/ $\text{SnO}_2$ [44], etc.).In addition, higher  $\text{pH}_{\text{PZC}}$  value which favored the adsorption of phenol molecules, and mixed valence states of metal elements to benefit the active electrode process as shown by equation 3 were proposed to be the other two factors to result in higher electrochemical catalytic activity of Cu-Ce/AC electrode. Therefore, as the synthesis result, the Cu-Ce/AC owns more remarkable electrochemical degradation performance of phenol than AC and Cu/AC. Hence, the conclusion can be obtained that doping Ce to activate carbon supported Cu/AC electrode could generate excellent catalytic activity for organic degradation also. Compared to the fore-mentioned metal(Ti/Ru) supported anode, the AC supported anode has the advantages including larger specific surface area, higher chemical and thermal stability, and lower cost. Therefore, the Cu-Ce/AC with considerable electro catalytic performance is a promising anode material for treatment of wastewaters containing organic compounds.

#### 4. CONCLUSIONS

The micro characterization revealed that oxides of Cu and Ce could be successfully loaded on the AC substrate. The Cu/Ce-AC had smaller crystal size average grains size and larger surface area, than that of Cu-AC. The existence of the redox couple  $\text{Cu}^{2+}/\text{Cu}$  and  $\text{Ce}^{4+}/\text{Ce}^{3+}$  in catalyst was proved. Comparison tests of electrochemical oxidation degradation for phenol by using AC, Cu/AC and Cu/Ce-AC composite anodes showed that Cu/Ce-AC was the most effective anode materials. The COD and TOC removal efficiencies could achieve 97.88% and 80.26% in 50min at initiate phenol concentration =504mg/L, temperature = 25°C, pH = 3.0 and  $j = 80 \text{ A}\cdot\text{m}^{-2}$ , respectively. The catalytic mechanism for phenol degradation process was proposed also. In summary, the smaller grain size, larger surface area, greater  $\text{pH}_{\text{PZC}}$  value, higher ability to gain more chemical adsorbed oxygen and

mixed valence states of metal elements to benefit the active electrode process synthetically resulted in its more excellent electrochemical degradation performance for phenol.

#### ACKNOWLEDGEMENTS

This work was supported by the National Natural Science Foundation of China (grant number. 51171067), and Shen Zhen Strategic Emerging Industry Development Special Fund Project (grant number JC201005310696A).

#### References

1. S. X. Yang, W.P. Zhu, J.B. Wang and Z.X. Chen, *J. Hazard. Mater.*, 153 (2008) 1248.
2. M. Kurian and D. Nair, *J. Environ. Chem. Eng.*, 2 (2014)63.
3. X. C. Song, Z. A. Yang, Y. F. Zheng and H. Y. Yin, *Curr. Nanosci.*, 9(2013) 128.
4. M. Din, A. T. Hameed and B. H. Ahmad, *J. Hazard. Mater.*, 161 (2009) 1522.
5. S. X. Yang, W. P. Zhu, Z. P. Jiang, Z. X. Chen and J. B. Wang, *Appl. Surf. Sci.*, 252 (2006) 8499.
6. A. Katsoni, H. T. Gomes, L.M. Pastrana-Martínez, J. L. Fariac, J. L. Figueiredo, D. Mantzavinos, and A. M.T. Silva, *Chem. Eng. J.*, 172 (2011) 634.
7. A. Cybulski, *Ind. Eng. Chem. Res.*, 46 (2007) 4007.
8. L. Z. Wang, Y. Zhao, S. X. Yang, B. Wu, P. Li and Y. M. Zhao, *Int. J. Electrochem. Sci.*, 11 (2016) 2401
9. Q. Zhuo, S. Deng, B. Yang, J. Huang and G. Yu, *Environ. Sci. Technol.*, 45(2011) 2973.
10. H. Lin, J.F. Niu, J.L. Xu, Y. Li and Y.H. Pan, *Electrochim. Acta*, 97 (2013) 167.
11. J. L. Chen, G. C. Chiou and C. C. Wu, *Desalination*, 264(2010)92.
12. G. Zhao, J. Gao W. Shi, M. Liu and D. Li, *Chemosphere*, 77(2009)188.
13. J. Cao, H. Zhao, F. Cao, J. Zhang and C. Cao, *Electrochim. Acta*, 54(2009) 2595.
14. Q. Bi, J. Q. Xue, C. B. Yang, L. H. Y, G. P. Li and X. Zhang, *Int. J. Electrochem. Sci.*, 11(2016)7412
15. L. H. Tran, P. Drogui, G. Mercier and J. F. Blais, *J Hazard Mater.*, 164(2009)1118.
16. E. Chatzisyneon, S. Fierro, I. Karafyllis, D. Mantzavinos, N. Kalogerakis and A. Katsaou-nis, *Catal Today*, 151(2010)185.
17. H. C. Arredondo Valdez, G. García Jiménez, S. Gutiérrez Granados and C. Ponce- De-León, *Chemosphere*, 89 (2012) 1195.
18. S. A. Alves, T. C. R. Ferreira, N. S. Sabatini, A. C. A. Trientini, F. L. Migliorini and M. R. Baldan, *Chemosphere*, 88(2012)155.
19. J. Kong, S. Shi, L. Kong, X. Zhu and J. Ni, *Electrochim. Acta*, 53(2007)2048.
20. Q. Z. Dai, H. Shen, Y. J. Xia, F. Chen, J. D. Wang and J. M. Chen, *Separation and Purification Technology*, 104 (2013) 9.
21. Y. Liu, H. Liu, J. Ma and J. Li, *J Hazard Mater.*, 213–214(2012)222.
22. S. A. Messele, O.S.G.P. Soares, J.J.M. Órfã, F. Stüber, C. Bengoa, A. Fortuny, A. Fabregat and J. Font, *Appl. Catal. B: Environ.*, 154–155 (2014) 329.
23. J. J. M. Órfão, A. I. M. Silva, J. C. V. Pereira, S. A. Barata, I. M. Fonseca, P. C. C. Faria and M. F. R. Pereira, *J. Colloid Interface Sci.*, 296 (2006) 480.
24. C. Zhang, M.H. Zhou, G. B. Ren, X. M. Yu, L. Ma, J. Yang and F. K. Yu, *Water Res.*, 70 (2015) 414.
25. R. M. Liou and S. H. Chen, *J. Hazard. Mater.*, 172 (2009) 498.
26. E. Brillas and C. A. Martínez-Huitle, *Applied Catalysis B: Environmental*, 166–167 (2015) 603.
27. C. A. Martínez-Huitle and E. Brillas, *Applied Catalysis B: Environmental*, 87 (2009) 105–145.
28. B. R. Wang, J. C. He, F. Q. Liu and L Ding, *Journal of Alloys and Compounds*, 693 (2017) 902.

29. X. C. Zheng, S. P. Wang, S. R. Wang, S. M. Zhang, W. P. Huang and S. H. Wu, *Mater. Sci. Eng. C.*, 25 (2005)516.
30. H. Z. Ma , Q. F. Zhuo and B. Wang, *Environ. Sci. Technol.*, 41 (2007) 7491.
31. Y. Liu and D. Z. Sun, *J. Hazard. Mater.*,143 (2007) 448.
32. S. J. Park, B. J. Kim, *J. Colloid. Interface. Sci.*, 292 (2005) 493.
33. Z. Zhang, R. Y. Yang, Y. S. Gao, Y. F. Zhao, J. Y. Wang, L. Huang, J. Guo, T. T. Zhou. P. Lu, Z. H. Guo and Q. Wang, *Scientific reports*, (2014)32.
34. S. S. Lin, C. L. Chen, D. J. Chang and C. C. Chen, *Water Res.* 36 (2002) 3009.
35. H. Chen, A. Sayari, A. Adnot and F. Larachi, *Appl. Catal. B: Environ.*, 32(2001) 195.
36. W. Li, S. Zhao , B. Qi , Y. Du, X.H. Wang and M. X. Huo, *Appl. Catal. B: Environ.*, 92 (2009) 333.
37. O. Simond, V. Schaller and C. Comninellis, *Electrochim. Acta*, 42(1997)2009.
38. D. W. Miwa, G. R. P. Malpass, S .A. S. Machado and A. J. Motheo, *Water Research*, 40 (2006) 3281.
39. A. Goyal and V. C. Srivastava, *Chemical Engineering Journal*, 325 (2017) 289.
40. E. Brillas, I. Sirés and M.A. Oturan, *Chem.Rev.*, 109 (2009) 6570.
41. N. Barhoumi, H. Olvera-Vargas, N. Oturan, D. Huguenot, A. Gadri, S. Ammar, E. Brillas and M. A. Oturan, *Applied Catalysis B: Environmental*, 209 (2017) 637.
42. X. Y. Duan, Y. Y. Zhao, W. Liu ,L. M. Chang and X. Li, *Journal of the Taiwan Institute of Chemical Engineers*, 45 (2014) 2975.
43. X. M. Chen , P. d. Yao, D. H. Wang and X. Z. Wu ,*Chemical Engineering Journal*, 147 (2009) 412.
44. Y. Liu, H. L. Liu, J. Ma and J. J. Li, *Electrochimica Acta*, 56 (2011) 1352.

© 2017 The Authors. Published by ESG ([www.electrochemsci.org](http://www.electrochemsci.org)). This article is an open access article distributed under the terms and conditions of the Creative Commons Attribution license (<http://creativecommons.org/licenses/by/4.0/>).